

Nickel, Zn and Cd localisation in seeds of metal hyperaccumulators using μ -PIXE spectroscopy

Anthony G. Kachenko^{a,*}, Naveen P. Bhatia^b, Rainer Siegele^b, Kerry B. Walsh^c, Balwant Singh^a

^a Faculty of Agriculture, Food and Natural Resources, The University of Sydney, Building A03, NSW 2006, Australia

^b Institute for Environmental Research, Australian Nuclear Science and Technology Organisation (ANSTO), PMB1, Menai, NSW 2234, Australia

^c Plant Sciences Group, Central Queensland University, Rockhampton, Qld 4702, Australia

ARTICLE INFO

Available online 12 March 2009

PACS:

89.60.–k

87.23.–n

Keywords:

Eco-physiology

Heavy metals

Elemental mapping

Hybanthus floribundus

Pimelea leptospermoides

Thlaspi caerulescens

ABSTRACT

Metal hyperaccumulators are a rare group of plant species that accumulate exceptionally high concentrations of metals in above ground tissues without showing symptoms of phytotoxicity. Quantitative localisation of the accumulated metals in seed tissues is of considerable interest to help understand the eco-physiology of these unique plant species. We investigated the spatial localisation of metals within seeds of Ni hyperaccumulating *Hybanthus floribundus* subsp. *adpressus*, *H. floribundus* subsp. *floribundus* and *Pimelea leptospermoides* and dual-metal (Cd and Zn) hyperaccumulating *Thlaspi caerulescens* using quantitative micro-proton induced X-ray emission (μ -PIXE) spectroscopy. Intact seeds were hand-sectioned, sandwiched between Formvar films and irradiated using the 3 MeV high energy heavy ion microprobe at ANSTO. Elemental maps of whole *H. floribundus* subsp. *adpressus* seeds showed an average Ni concentration of 5.1×10^3 mg kg⁻¹ dry weight (DW) with highest Ni concentration in cotyledonary tissues (7.6×10^3 mg kg⁻¹ DW), followed by the embryonic axis (4.4×10^3 mg kg⁻¹ DW). Nickel concentration in whole *H. floribundus* subsp. *floribundus* seeds was 3.5×10^2 mg kg⁻¹ DW without a clear pattern of Ni localisation. The average Ni concentration in whole *P. leptospermoides* seeds was 2.6×10^2 mg kg⁻¹ DW, and Ni was preferentially localised in the embryonic axis (4.3×10^2 mg kg⁻¹ DW). In *T. caerulescens*, Cd concentrations were similar in cotyledon (4.5×10^3 mg kg⁻¹ DW) and embryonic axis (3.3×10^3 mg kg⁻¹ DW) tissues, whereas Zn was highest in cotyledonary tissues (1.5×10^3 mg kg⁻¹ DW). In all species, the presence of the accumulated metal within the cotyledonary and embryonic axis tissues indicates that the accumulated metal was able to move apoplastically within the seed.

© 2009 Elsevier B.V. All rights reserved.

1. Introduction

Ultramafic soils are naturally occurring metalliferous environments that are host to the majority of metal hyperaccumulating plant species [1]. This rare group of plants possess specialised physiological mechanisms that enable them to actively accumulate metals in their above-ground tissues [2,3]. To classify plants as metal hyperaccumulators, the concentration(s) of metals accumulated must exceed threshold concentration with no toxicity symptoms or reduction in growth. For example, for cadmium (Cd), nickel (Ni) and zinc (Zn) hyperaccumulators threshold concentrations have been suggested to be more than 100 mg kg⁻¹, 1000 mg kg⁻¹ and 10,000 mg kg⁻¹ dry weight (DW), respectively [3].

In the past decade, interest in elucidating the intriguing physiological mechanisms that contribute to detoxification of the accumulated metals in hyperaccumulating plants has grown many

folds. The cellular distribution of the accumulated metals has been investigated using a variety of microscopy techniques, namely energy dispersive X-ray analysis (EDXA) and micro-proton induced X-ray emission (μ -PIXE) spectroscopy [4–15]. The latter technique is considered a reliable, micro-analytical tool, offering high sensitivity and accuracy for quantitative elemental mapping in hyperaccumulating plant tissues [16]. The majority of these studies have explored above-ground tissues, in particular leaves, which act as the major sink for the accumulated metal(s). These studies suggest that epidermal tissue act as depositories of the accumulated metals [5,6,11], however, this pattern of localisation is not universal among all metal hyperaccumulators. For example, Fernando et al. [9], using μ -PIXE spectroscopy, observed that manganese (Mn) was preferentially localised in the palisade mesophyll of Mn hyperaccumulators *Gossia bidwillii* and *Vrota neurophylla*. Cellular localisation in leaf tissues appears to be a species-specific metal detoxification phenomenon.

Similarly, the spatial distribution of metals accumulated within seed (fruit) tissue of metal hyperaccumulating plants is unclear.

* Corresponding author. Tel.: +61 2 9351 2917; fax: +61 2 9351 5108.
E-mail address: a.kachenko@usyd.edu.au (A.G. Kachenko).

For example, Bhatia et al. [8] employed μ -PIXE to study the seeds of Ni hyperaccumulator *Stackhousia tryonii* and reported the highest Ni concentration in the seed wall (pericarp; 4,433 mg kg⁻¹ DW) with a fraction of Ni being accumulated within endospermic (309 mg kg⁻¹ DW) and cotyledonary (182 mg kg⁻¹ DW) tissues. In contrast, Sagner et al. [15] using EDXA reported the highest Ni concentration in the endosperm (14,000 mg kg⁻¹ DW) and pulp tissues (mesocarp; 8,000 mg kg⁻¹ DW) of Ni hyperaccumulator *Sebertia acuminata*. In Ni hyperaccumulating *Thlaspi pindicum* seeds, preferential localisation was reported in the micropylar area opposite the radicle and in the epidermis of cotyledons, relative to the mesophyll [13]. A similar patterns has also been reported in Cd hyperaccumulator *T. praecox* [12]. An evolutionary explanation of metal compartmentation in seeds was offered by Bhatia et al. [8]. The authors suggested that localisation in the pericarp might deter herbivores and/or provide protection against pathogen attack. However, the localisation pattern observed in *Sebertia acuminata*, *T. pindicum* and *T. praecox* does not support this hypothesis [12,13,15].

In this study we employed μ -PIXE spectroscopy to investigate cellular compartmentation of Ni in three Australian, serpentine-endemic Ni hyperaccumulators: *Hybanthus floribundus* subsp. *adpressus* E.M. Benn. (family Violaceae), *H. floribundus* (Lindl.) F. Muell. subsp. *floribundus* and *Pimelia leptospermoides* (family Thymelaeaceae) [6,17]. We also report on the cellular compartmentation of Cd and Zn in seeds of dual-hyperaccumulating *Thlaspi caerulescens* J. & C. Presl (family Brassicaceae), commonly found on serpentine and non-metalliferous soils in temperate climates [18,19]. To our knowledge, the presence of metals and elemental localisation in these seeds has not been previously explored using μ -PIXE spectroscopy.

2. Materials and methods

2.1. Seed material

Air-dry *H. floribundus* subsp. *adpressus* seeds were procured from Nindethana Seed Company (Albany, Western Australia). The seeds were collected from a population near Ravensthorpe, Western Australia in 1988. Seeds of *H. floribundus* subsp. *floribundus* were procured from Kings Park Botanic Garden (West Perth, Western Australia). Seeds were sourced from a population near Angus Corner, Great Victorian Desert, Western Australia in 2002. *Pimelia leptospermoides* seeds were collected from uprooted, abandoned plants near Mt Wheeler, Queensland in 2001. Seeds of *T. caerulescens* were supplied by the Late Prof. R.R. Brooks (New Zealand) in 1999.

2.2. Sample preparation

In this study, seeds were prepared as described by Bhatia et al. [8]. Briefly, seeds were cut longitudinally with a stainless steel razor blade and sandwiched between Formvar (in 2% w/v ethylene dichloride) films. Samples were then mounted onto aluminium target holders [8] and stored in a desiccator until analysis. To avoid redistribution of the elements, seeds were used unwashed prior to μ -PIXE investigation.

2.3. Micro-PIXE analysis

Nuclear microprobe analyses were performed on three independent seed samples from each species using the 10 MV Tandem accelerator at the Australian Nuclear Science and Technology Organization [20]. A proton beam of 3 MeV energy and current of 200–1000 pA was focused with a typical spot size of between 3 and 5 μ m. A high purity Ge detector with a 100 mm² active area,

located 33 mm from the sample was used to acquire μ -PIXE spectra. To reduce low energy X-rays and thus pile-up in the μ -PIXE spectrum, a 100 μ m Mylar foil was positioned in front of the detector to attenuate X-rays from the light elements. The proton beam was scanned over samples up to a maximum of 2.5 \times 2.5 mm² and samples were typically irradiated with a total charge between 2 and 5 μ C. Further details regarding microprobe calibration and data acquisition have been presented elsewhere [8]. List-mode data files were collected using OM_DAO and all further data analyses were performed using the GeoPIXE II software package [21]. True elemental maps were generated using a Dynamic Analysis (DA) matrix transform method of GeoPIXE II [22]. Region selection analysis (RSA) using the DA method was used to extract representative concentration data and minimum detection limits from select regions (*viz.* testa, cotyledons and embryonic axis) within seed sections from on-screen quantitative distribution maps. Owing to the low resolution of elemental maps, the selected regions contained grouped cell types. For example, the embryonic axis consisted of the epicotyl, hypocotyl and radicle. In addition, transects were drawn across elemental maps using quantitative point analysis (QPA) based on the DA method in order to provide a typical elemental profile across plant sections [7]. GenStat version 8.1.0.152 [23] was used for the statistical analysis of RSA results. Data were subjected to ANOVA and Fisher's LSD's were calculated to separate the means at a 95% level of significance ($P \leq 0.05$).

3. Results

Amongst whole seed sections of *H. floribundus* subsp. *adpressus*, subsp. *floribundus* and *P. leptospermoides*, the concentration of Ni, Ca and K, as determined by RSA, followed the order K > Ca > Ni (Fig. 1; Table 1). The Ni hyperaccumulation level (i.e. 1.0 \times 10³ mg kg⁻¹ DW) was exceeded in only *H. floribundus* subsp. *adpressus* seeds with 5.1 \times 10³ mg kg⁻¹ DW in whole seed sections (Table 1). Elemental maps generated from whole seed sections of *H. floribundus* subsp. *adpressus* and *P. leptospermoides* revealed a variable pattern of localisation that was not uniform (Fig. 1). In *H. floribundus* subsp. *adpressus*, the Ni concentration was highest in the cotyledons (7.6 \times 10³ mg kg⁻¹ DW) while in *P. leptospermoides*, highest Ni concentration of 4.3 \times 10² mg kg⁻¹ DW occurred in the embryonic axis (Table 1). In both species, lowest Ni concentration occurred in the testa, which was confirmed by quantitative point analysis (QPA) profiles across seed sections (Table 1; Fig. 3). In contrast, concentration of Ni in *H. floribundus* subsp. *floribundus* was statistically alike amongst tissue types, and ranged from 2.2 \times 10² mg kg⁻¹ DW in the testa to 4.8 \times 10² mg kg⁻¹ DW in the embryonic axis (Table 1; Fig. 3).

An examination of elemental maps generated from whole seed sections of *Thlaspi caerulescens* revealed that the concentrations of Cd and Zn were not uniform amongst tissues (Fig. 2). Cadmium concentration in whole seed sections was 32-folds higher than the hyperaccumulation level (i.e. 1.0 \times 10² mg kg⁻¹ DW), however Zn concentration did not reach the hyperaccumulation level (i.e. 1.0 \times 10⁴ mg kg⁻¹ DW). The concentration of Cd and Zn was lowest in the testa with concentration of 1.0 \times 10³ mg kg⁻¹ DW and 4.4 \times 10² mg kg⁻¹ DW, respectively (Table 1). In the cotyledons, QPA revealed a peak Cd and Zn concentration of 3.7 \times 10⁴ and 2.0 \times 10⁴ mg kg⁻¹ DW, respectively (Fig. 3).

4. Discussion

The preferential localisation of Ni in *H. floribundus* subsp. *adpressus* and *P. leptospermoides* embryonic tissues (cotyledons and embryonic axis) suggests the possibility of apoplastic movement within seeds. The same reasoning may also explain the

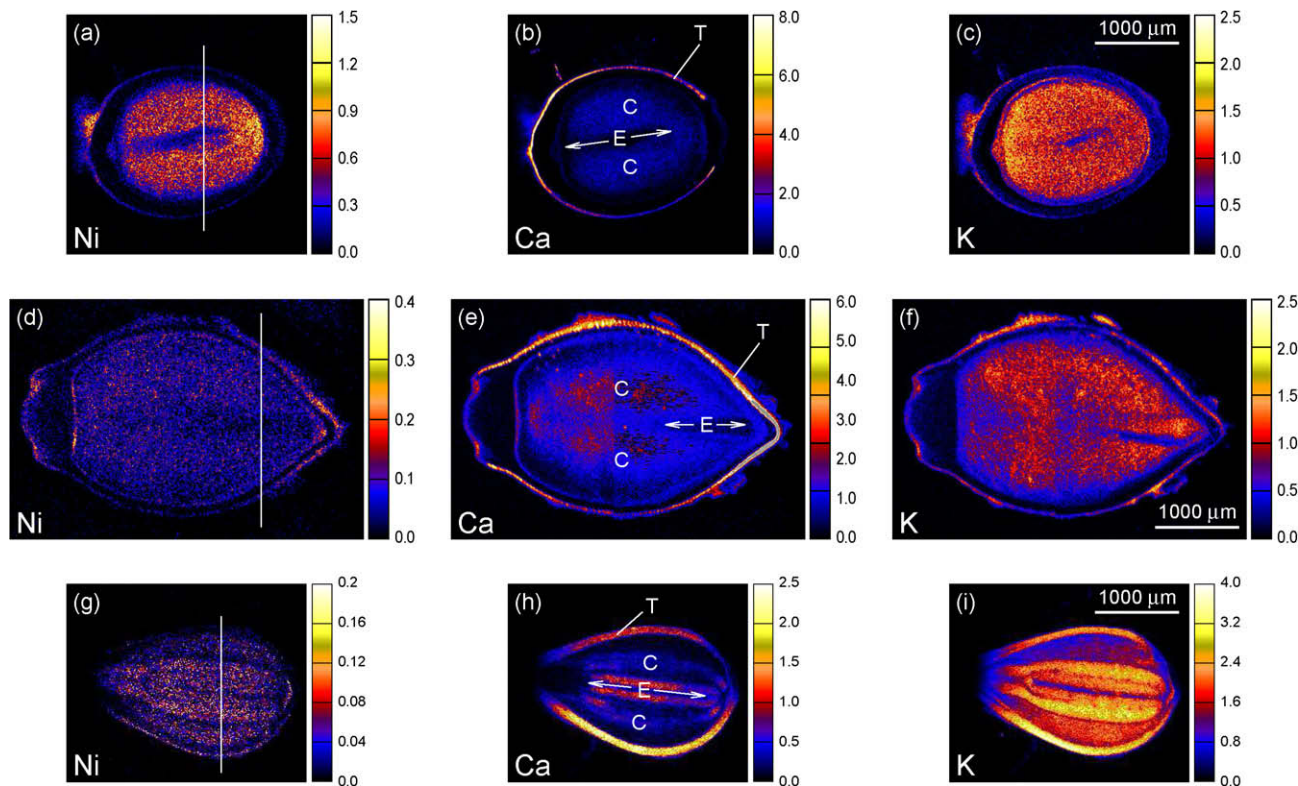


Fig. 1. Quantitative elemental maps showing distribution of Ni, Ca and K in air-dried seed longitudinal sections of *Hybanthus floribundus* subsp. *adpressus* (a)–(c), *H. floribundus* subsp. *floribundus* (d)–(f) and *Pimelea leptospermoides* (g)–(i). Concentrations are in dry weight %. The transect outlined on Ni images relates to quantitative point analysis (QPA) across seeds in Fig. 3. Where T, testa; C, cotyledon and E, embryonic axis.

preferential localisation of Cd and Zn observed in the embryonic tissues of dual-hyperaccumulating *T. caerulescens*, and corroborate with the results reported for seeds of Ni hyperaccumulating *T. pindicum* [13] and Cd/Zn dual-hyperaccumulator *T. praecox* [12]. For example, in *T. praecox* seeds, Cd was preferentially localised along the embryonic axis, with Cd concentrations in the seed tissue following the order: epidermis ($1,797 \text{ mg kg}^{-1}$) > mesophyll (784 mg kg^{-1}) > aleurone (444 mg kg^{-1}) > testa (47.8 mg kg^{-1}). These authors suggested that a transporter protein with a high affinity for Cd assisted in the transport of Cd into the embryonic tissues, particularly in the later stage of embryo development in *T. pindicum*. Transporter proteins have been suggested to play a role in metal uptake and homeostasis in hyperaccumulator plants, as reported in the Cd/Zn hyperaccumulator *T. caerulescens* [24] and the Ni hyperaccumulator *T. goesingense* [25]. However, to our knowledge, their expression within seeds of hyperaccumulators remains unknown.

Our results are in direct contrast with those of Bhatia et al. [8] who observed highest Ni localisation in the fruit wall (pericarp;

4433 mg kg^{-1} DW) of Ni hyperaccumulator *S. tryonii*. These authors indicated that Ni movement was principally symplastic within fruit tissues owing to the lack of symplastic attachment between the filial generation (i.e. embryo and endosperm) and the parent. This reasoning is in contrast with the observation of Sagner et al. [15] who reported highest concentration of Ni in the rudimentary endosperm of Ni hyperaccumulating *S. acuminata* fruit ($14,000 \text{ mg kg}^{-1}$ DW). Similarly, in Zn tolerant *Biscutella laevigata* seeds, highest concentration of Zn was found in the endosperm, and least in the testa, with concentration of 414 and 44 mg kg^{-1} DW, respectively [26]. These authors postulated that the endosperm layer beneath the testa may act as a barrier, preventing Zn from entering into embryonic tissues.

Despite the uniform pattern of Ni localisation within *H. floribundus* subsp. *floribundus* seed tissues, the presence of Ni within the embryonic axis suggests apoplastic movement of Ni. Compared to subsp. *adpressus*, the low concentration of Ni in whole seed sections of subsp. *floribundus* is likely to be a result of the differences in Ni hyperaccumulation amongst the parent plants (i.e. source of

Table 1
Nickel concentration (mg kg^{-1} DW) within seed sections of *Hybanthus floribundus* subsp. *adpressus*, *H. floribundus* subsp. *floribundus*, *Pimelea leptospermoides*; and Cd and Zn concentration (mg kg^{-1} DW) within seed sections of *Thlaspi caerulescens*. Concentrations (means \pm SE) were determined following dynamic analysis of individually selected regions of three replicate seeds. Different letters within the same column indicate a significant difference ($P \leq 0.05$). Minimum detection limit (MDL; mg kg^{-1} DW) of each measurement is also presented.

Seed part analysed	<i>Hybanthus</i> subsp. <i>adpressus</i>		<i>Hybanthus floribundus</i> subsp. <i>floribundus</i>		<i>Pimelea leptospermoides</i>		<i>Thlaspi caerulescens</i>		<i>Thlaspi caerulescens</i>	
	mg Ni kg^{-1} DW	MDL	mg Ni kg^{-1} DW	MDL	mg Ni kg^{-1} DW	MDL	mg Cd kg^{-1} DW	MDL	mg Zn kg^{-1} DW	MDL
Whole section	$5.1 \pm 1.2 \times 10^3$ ^b	5	$3.5 \pm 0.9 \times 10^2$ ^a	2	$2.6 \pm 0.3 \times 10^2$ ^b	2	$3.2 \pm 0.8 \times 10^3$ ^b	31	$1.1 \pm 0.06 \times 10^3$ ^{bc}	3
Seed coat (testa)	$1.0 \pm 0.2 \times 10^3$ ^a	11	$2.2 \pm 0.6 \times 10^2$ ^a	6	$1.0 \pm 0.3 \times 10^2$ ^a	4	$1.0 \pm 0.4 \times 10^3$ ^a	58	$4.4 \pm 0.08 \times 10^2$ ^a	5
Cotyledons	$7.6 \pm 2.0 \times 10^3$ ^c	6	$4.0 \pm 0.9 \times 10^2$ ^a	4	$2.8 \pm 0.06 \times 10^2$ ^b	6	$4.5 \pm 1.5 \times 10^3$ ^b	54	$1.5 \pm 0.1 \times 10^3$ ^c	4
Embryonic axis	$4.4 \pm 1.1 \times 10^3$ ^b	14	$4.8 \pm 0.9 \times 10^2$ ^a	6	$4.3 \pm 0.5 \times 10^2$ ^c	3	$3.3 \pm 0.6 \times 10^3$ ^b	72	$1.0 \pm 0.3 \times 10^3$ ^b	6

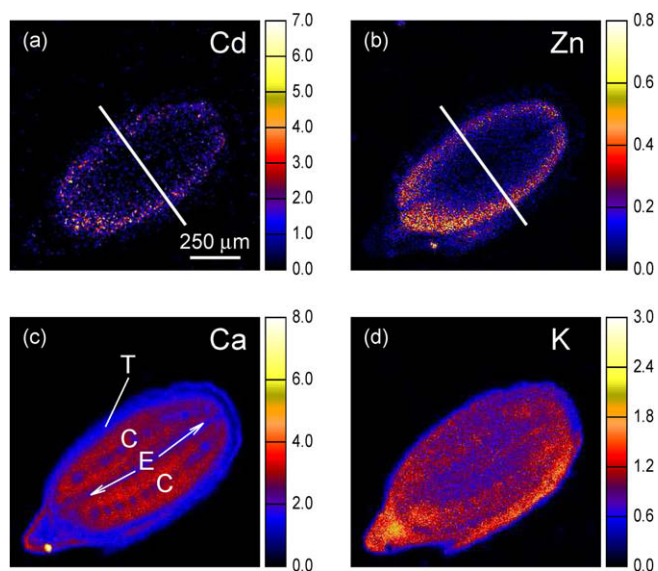


Fig. 2. Quantitative elemental maps showing distribution of Cd (a), Zn (b), Ca (c) and K (d) in an air-dried seed longitudinal section of *Thlaspi caerulescens*. Concentrations are in dry weight %. The transects outlined in the Cd and Zn images relate to quantitative point analysis (QPA) across seed in Fig. 3. Where T, testa; C, cotyledon and E, embryonic axis.

seed material). Reportedly, subsp. *floribundus* is a facultative species, i.e. inhabiting both ultramafic as well as non-ultramafic soils, whereas subsp. *adpressus* is an obligate species, restricted only to nickeliferous soils [27–29]. *Pimelia leptospermoides* is also an obligate species on ultramafic soils and has been reported to accumulate variable levels of Ni (21–1620 mg kg⁻¹ DW) in its above-ground tissue [30]. Owing to this behaviour, *P. leptospermoides* is considered a ‘marginal’ hyperaccumulator, and like subsp. *floribundus*, low Ni concentration in whole seed section may reflect low Ni concentration in parent plants [31]. However, in both species, insufficient data is available to elucidate the precise factors that might influence the observed level of Ni concentration in seeds.

Zinc concentration in *T. caerulescens* seeds did not reach the threshold concentration used to classify it as a Zn hyperaccumulator; however, Cd accumulation exceeded the 100 mg kg⁻¹ DW threshold concentration. These results are in agreement with those of Vogel-Mikuš et al. [12] who reported Cd but not Zn hyperaccumulation in *T. praecox* seeds. These authors suggested that enhanced Cd mobility throughout the plant tissues, and increased phloem loading during seed development, may be related to ineffective Cd compartmentalization in the parent plant. This explanation requires further investigations to elucidate the precise physiological mechanisms of Cd/Zn loading into seeds of dual-hyperaccumulator *T. caerulescens*.

Amongst the studied hyperaccumulators, an eco-physiological explanation to validate the transfer of metals from parent plants into developing seeds is not immediately apparent. In *Hybanthus* subspecies, studies have indicated difficulties in propagating seed material and it is possible that elevated Ni concentration in seeds may hinder their successful germination [32,33]. Bhatia et al. [8] indicated that the high levels of Ni in *S. tryonii* pericarp tissues may deter herbivores, however this explanation does not support the results in the present study. A plausible explanation was offered by Vogel-Mikuš et al. [12] who suggested that compartmentation of Cd and Zn in *T. praecox* cotyledonary epidermal tissues might protect ancestral photosynthetic tissues of the expanded cotyledons. Irrespective of the localisation pattern of the accumulated metal, the presence of elevated concentrations in seeds suggest that hyperaccumulators in the early stages of development

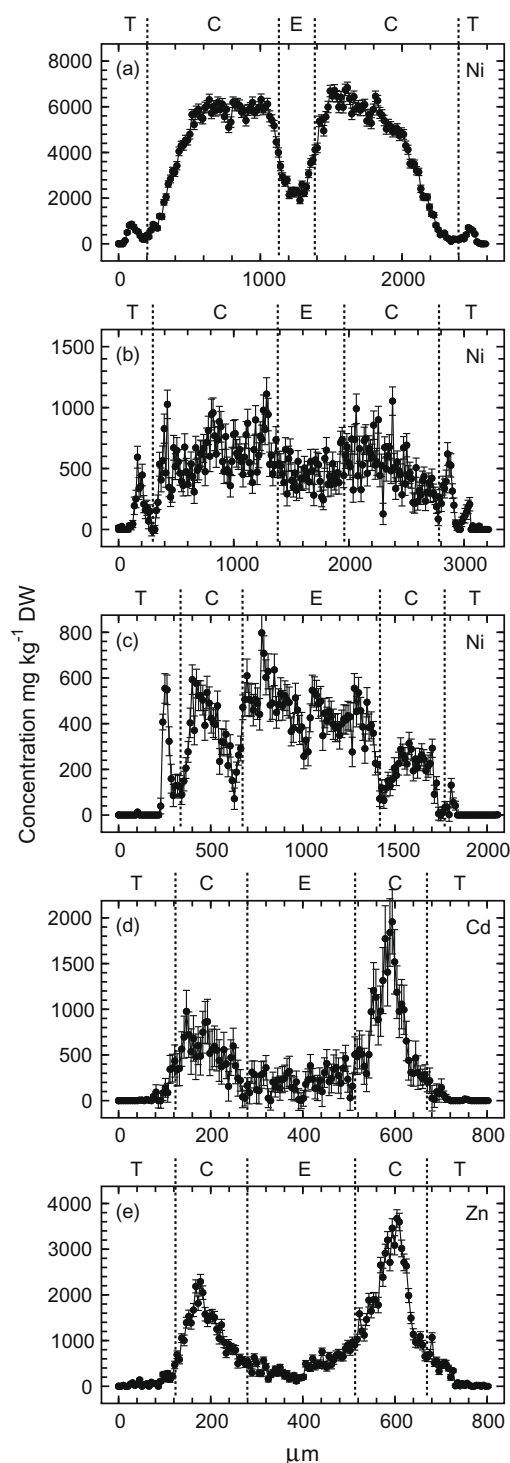


Fig. 3. Quantitative point analysis (QPA) profiles derived from the micro-PIXE analysis of *Hybanthus floribundus* subsp. *adpressus*, (a), *H. floribundus* subsp. *floribundus* (b) and *Pimelea leptospermoides* (c) and *Thlaspi caerulescens* (d–e). The profiles correspond to the typical transects outlined in Figs. 1 and 2. Statistical errors of each point are indicated on the profile. Where T, testa; C, cotyledon and E, embryonic axis.

will already contain some accumulated metal, however, the majority of metal uptake will occur post-emergence.

Acknowledgements

We acknowledge the Australian Institute of Nuclear Science and Engineering for financial assistance (AWARD No. AINGRA 04161).

Anthony Kachenko was supported by an APA scholarship from the Australian Commonwealth Government.

References

- [1] R.D. Reeves, A.J.M. Baker, in: I. Raskin, B.D. Ensley (Eds.), *Phytoremediation of Toxic Metals: Using Plants to Clean Up the Environment*, John Wiley and Sons Inc., New York, USA, 2000, p. 193.
- [2] J.L. Hall, *J. Exp. Bot.* 53 (2002) 1.
- [3] A.J.M. Baker, S.P. McGrath, R.D. Reeves, J.A.C. Smith, in: N. Terry, G. Bañuelos (Eds.), *Phytoremediation of Contaminated Soil and Water*, CRC Press, Boca Raton, 2000, p. 85.
- [4] A.G. Kachenko, N.P. Bhatia, B. Singh, R. Siegele, *Plant Soil* 300 (2007) 207.
- [5] A.G. Kachenko, R. Siegele, N.P. Bhatia, B. Singh, M. Ionescu, *Nucl. Instr. and Meth. B* 266 (2008) 1598.
- [6] A.G. Kachenko, B. Singh, N.P. Bhatia, R. Siegele, *Nucl. Instr. and Meth. B* 266 (2008) 667.
- [7] N.P. Bhatia, K.B. Walsh, I. Orlic, R. Siegele, N. Ashwath, A.J.M. Baker, *Funct. Plant Biol.* 31 (2004) 1061.
- [8] N.P. Bhatia, I. Orlic, R. Siegele, N. Ashwath, A.J.M. Baker, K.B. Walsh, *New Phytol.* 160 (2003) 479.
- [9] D.R. Fernando, E.J. Bakkaus, N. Perrier, A.J.M. Baker, I.E. Woodrow, G.N. Batianoff, R.N. Collins, *New Phytol.* 171 (2006) 751.
- [10] H. Küpper, E. Lombi, F.J. Zhao, G. Wieshammer, S.P. McGrath, *J. Exp. Bot.* 52 (2001) 2291.
- [11] S.M. Heath, D. Southworth, J.A. D'allura, *Int. J. Plant Sci.* 158 (1997) 184.
- [12] K. Vogel-Mikuš, P. Pongrac, P. Kump, M. Necemer, J. Simcic, P. Pelicon, M. Budnar, B. Povh, M. Regvar, *Environ. Pollut.* 147 (2007) 50.
- [13] G.K. Psaras, Y. Manetas, *Ann. Bot.* 88 (2001) 513.
- [14] W.J. Przybyłowicz, C.A. Pineda, V.M. Prozesky, J. Mesjasz-Przybyłowicz, *Nucl. Instr. and Meth. B* 104 (1995) 176.
- [15] S. Sagner, R. Kneer, G. Wanner, J. Cossons, D. Deus-Neumann, M.H. Zenk, *Phytochemistry* 47 (1998) 339.
- [16] W.J. Przybyłowicz, J. Mesjasz Przybyłowicz, C.A. Pineda, C.L. Churms, C.G. Ryan, V.M. Prozesky, R. Frei, J.P. Slabbert, J. Padayachee, W.U. Reimold, *X-ray Spectrom.* 30 (2001) 156.
- [17] G.N. Batianoff, R.L. Specht, in: A.J.M. Baker, J. Proctor, R.D. Reeves (Eds.), *The Vegetation of Ultramafic (Serpentine) Soils*, Intercept Ltd., Andover UK, 1992, p. 109.
- [18] J. Escarré, C. Lefèbvre, W. Gruber, M. Leblanc, J. Lepart, Y. Rivière, B. Delay, *New Phytol.* 145 (2000) 429.
- [19] A.G.L. Assunção, P.M. Bleeker, W.M. ten Bookum, R. Vooijs, H. Schat, *Plant Soil* 303 (2007) 289.
- [20] R. Siegele, D.D. Cohen, N. Dytlewski, *Nucl. Instr. and Meth. B* 158 (1999) 31.
- [21] C.G. Ryan, E. van Achterbergh, C.J. Yeats, T. Tin Win, G. Cripps, *Nucl. Instr. and Meth. B* 189 (2002) 400.
- [22] C.G. Ryan, E. van Achterbergh, D.N. Jamieson, *Nucl. Instr. and Meth. B* 231 (2005) 162.
- [23] R.W. Payne, S.A. Harding, D.A. Murray, D.M. Soutar, D.B. Baird, S.J. Welham, A.F. Kane, A.R. Gilmour, R. Thompson, R. Webster, *GENSTAT Release 8 Reference Manual*, VSN International, Oxford, UK, 2005.
- [24] E. Lombi, E.J. Zhao, S.P. McGrath, S.D. Young, G.A. Sacchi, *New Phytol.* 149 (2001) 53.
- [25] D.E. Salt, *In Vitro Cell. Dev. Biol. Plant* 37 (2001) 326.
- [26] J. Mesjasz Przybyłowicz, K. Grodzińska, W.J. Przybyłowicz, B. Godzik, G. Szarek-Łukaszewska, *Nucl. Instr. and Meth. B* 181 (2001) 634.
- [27] E.M. Bennett, *Nuytsia* 1 (1972) 218.
- [28] B.C. Severne, *Nature* 248 (1974) 807.
- [29] B.C. Severne, R. Brooks, *Planta* 103 (1972) 91.
- [30] G.N. Batianoff, R.D. Reeves, R.L. Specht, in: T. Jaffré, R.D. Reeves, T. Becquer (Eds.), *Écologie des milieux sur roches ultramafiques et sur sols métallifères*, Documents Scientifiques et Techniques, ORSTOM, Noumea, New Caledonia, 1997, p. 147.
- [31] R.D. Reeves, *Plant Soil* 249 (2003) 57.
- [32] S. Roche, K. Dixon, J. Pate, *Aust. J. Bot.* 45 (1997) 783.
- [33] S.D. Bidwell, PhD, The University of Melbourne, 2001.